

## Theoretical Study of Adsorption and Diffusion of Group IIIA Metals on Si(111)

Demeter Tzeli,\* Ioannis D. Petsalakis, and Giannoula Theodorakopoulos

*Theoretical and Physical Chemistry Institute, National Hellenic Research Foundation, 48 Vassileos Constantinou Ave., Athens 116 35, Greece**Received: April 13, 2009; Revised Manuscript Received: June 4, 2009*

Adsorption of group IIIA elements (M = B, Al, Ga, and In) on a model Si(111) surface was studied by density functional theory calculations. Eight stable structures were determined for the M adsorbed species. The incorporation of the M atoms on the Si surface is investigated, and the energy barriers for the incorporation are calculated. The binding energy of the lowest calculated minimum of chemisorbed M at Si(111), after correcting for the basis set superposition error, is 6.3 (B, S<sub>5</sub> substitutional site), 3.4 (Al, T<sub>4</sub> adsorption site), 2.9 (Ga, T<sub>4</sub>), and 2.5 (In, T<sub>4</sub>) eV. Our results are in good agreement with previous experimental work, where available. The activation energy barrier from the T<sub>4</sub> to the H<sub>3</sub> adsorption site is 1.2 (Al), 1.1 (Ga), and 0.7 eV (In); the activation energy barrier from the lowest energy structure with M connected to the surface at a dangling bond to a precursor of T<sub>4</sub> is 0.5 (B), 1.6 (Al), 1.7 (Ga), and 1.9 eV (In).

## I. Introduction

Adsorption and diffusion of the group IIIA metals on Si surfaces have attracted much attention in recent decades due to its technological importance for potential applications for atomic-scale devices, catalyst, and low-cost mass production of group-IIIa-based devices.<sup>1</sup> When a metal is adsorbed on a semiconductor surface, the surface undergoes some structural changes which depend sensitively on the interaction between the metal adsorbate and the semiconductor surface. The microscopic morphology and the dynamics of the chemisorbed atom–surface system can provide important information on the selection of the appropriate adsorbate for a specific application.

There are many experimental and theoretical studies (mostly band structure calculations) on the adsorption of group IIIA, i.e., B,<sup>2–7</sup> Al,<sup>8–22</sup> Ga,<sup>14,15,22–32</sup> and In<sup>13–15,17,21,23,33–44</sup> on Si(111) surface, concerning the geometric and electronic structure, the surface changes associated with metal diffusion on the surface, the growth of group IIIA films on Si(111), and the properties induced by the adsorption of M on the Si(111) surface.

It is known that adsorption of group IIIA metals on Si(111) induces a ( $\sqrt{3} \times \sqrt{3}$ )R30° reconstruction at 1/3 monolayer coverage, with B occupying a substitutional S<sub>5</sub> site, lying directly below a Si adatom at a T<sub>4</sub> site,<sup>3</sup> while in the case of Al, Ga, and In the metal atoms occupy T<sub>4</sub> sites.<sup>3,6,8,15</sup> The interaction of B with Si(111) and the proposition of the S<sub>5</sub> site as the lowest-energy structure has been verified experimentally using synchrotron X-ray diffraction,<sup>2</sup> low-energy electron diffraction (LEED),<sup>3</sup> scanning tunneling microscopy (STM),<sup>4,6</sup> atom-resolved tunneling spectroscopy,<sup>4</sup> and photoemission.<sup>4</sup> In addition calculations have been carried out for the S<sub>5</sub> and T<sub>4</sub> adsorption sites for B atoms, employing pseudopotential local density functional theory with a plane wave basis and slab configuration,<sup>6</sup> as well as Hartree–Fock (HF) and density functional theory (DFT) on a Si cluster.<sup>7</sup> Lyo et al.<sup>6</sup> showed that, at low temperatures, B adsorbs as an adatom in a T<sub>4</sub> site, but it is not the lowest energy structure and with proper annealing B occupies a subsurface substitutional site directly below the Si adatom.

First, in 1984, Northrup<sup>8</sup> studied the Si(111)( $\sqrt{3} \times \sqrt{3}$ )R30°–Al surface by first principles pseudopotential total energy with a plane wave basis and proposed that Al occupies a T<sub>4</sub> site and this structure is lower in energy than the H<sub>3</sub> model. Since then theoretical studies on the T<sub>4</sub>, H<sub>3</sub>, and T<sub>1</sub> model have been carried out employing HF,<sup>9,10</sup> configuration interaction (CI),<sup>9</sup> and second order Møller–Plesset perturbation theory (MP2)<sup>10</sup> using small AlSi<sub>m</sub>H<sub>n</sub> clusters up to 26 atoms for the SCF calculation and up to 16 atoms for CI and MP2 and extrapolation to larger clusters up to 49 atoms<sup>10</sup> with partial geometry optimization on a AlSi<sub>5</sub> subcluster. DFT calculations carried out on the T<sub>1</sub> model using a Si<sub>10</sub>Al model and studying the effect of an external electric field.<sup>11</sup> Moreover, band structure calculations with the Car–Parrinello method were applied on T<sub>4</sub> and H<sub>3</sub>.<sup>20</sup> In 1999 Hoshino et al.<sup>12a</sup> calculated the migration process of an Al adatom on the Si(111) surface from T<sub>4</sub> to the H<sub>3</sub> site employing DFT calculations and a Si<sub>n</sub>H<sub>m</sub>Al cluster ranging from 18 atoms to 71 atoms. Experimentally, the adsorption of the Al at Si(111) has been studied by inverse-photoemission spectroscopy,<sup>15</sup> STM,<sup>16,17</sup> and LEED.<sup>18</sup>

Experimentally the adsorption of Ga at Si(111), its growth and geometry and the properties induced to the surface have been studied by LEED,<sup>23,26,28</sup> Auger electron spectroscopy (AES),<sup>23</sup> photoemission spectroscopy,<sup>15,23</sup> STM,<sup>24,29</sup> reflection high energy electron diffraction (RHEED),<sup>25</sup> synchrotron radiation photoelectron spectroscopy,<sup>26</sup> angle-resolved photoemission spectroscopy (ARPES),<sup>27</sup> and X-ray standing wave technique.<sup>30</sup> Theoretically, adsorption of Ga at Si(111) has been studied with pseudopotential method based on the DFT, local density approximation, with a plane wave basis and slab configuration,<sup>15,22,29,31</sup> HF cluster calculation,<sup>30</sup> and molecular dynamics.<sup>32</sup> Data are reported mainly for the T<sub>4</sub> and/or the H<sub>3</sub> adsorption sites. Additionally, Thundat et al.<sup>30</sup> report data also for the T<sub>1</sub> and S<sub>5</sub> adsorption sites. Finally, Cho et al.<sup>31</sup> give data in total for 6 adsorption sites and Lee et al.<sup>14</sup> for 7 adsorption sites above the Si(111) surface around the Si rest atom.

Finally, adsorption of In at Si(111), indium induced reconstructions, diffusion, and desorption have been studied by LEED,<sup>21,43</sup> RHEED,<sup>33,34</sup> STM,<sup>35,41,42,44</sup> impact collision ion scattering spectroscopy,<sup>36</sup> perturbed  $\gamma\gamma$  angular correlation

\* Corresponding author. Fax: +30-210-7273-794. E-mail: dtzeli@eie.gr.

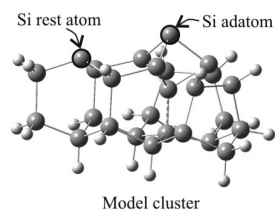
spectroscopy (PAC),<sup>37</sup> X-ray diffraction study,<sup>38</sup> scanning tunneling spectroscopy (STS),<sup>42</sup> electron energy loss spectroscopy,<sup>43</sup> AES,<sup>43</sup> high resolution photoelectron spectroscopy,<sup>44</sup> and inverse-photoemission spectroscopy.<sup>15</sup> As far as we know, only two theoretical studies exist for this system employing band structure calculations.<sup>14,15</sup>

From the above it is obvious that a great deal of work, both experimental and theoretical, has been devoted to the adsorption of group IIIA metal atoms (mostly on Al and Ga) at Si(111). However, nearly all theoretical studies on the M–Si(111) systems, mentioned above, are focused on the geometry in the equilibrium conditions for the most stable adsorption site of M atoms, with widely differing values of the reported binding energies (see below), and little is known about other adsorption sites of M atoms, the migration process among different chemisorbed structures, or the energy barriers between different stable structures. For the last topic, only one study exists involving chemisorbed Al, where the energy barrier between two stable structures has been calculated.<sup>12a</sup> An adequate comprehension of the dynamics of group IIIA metal atom adsorption at Si(111) would require a systematic and consistent mapping of the different stable structures as well as energy barriers, and this is the purpose of the present work.

In the present study, we report the results of a systematic investigation of the interaction of group IIIA metal atoms M, M = B, Al, Ga, and In, with the reconstructed Si(111) surface at very low coverage. Using the same methodology as in our previous studies<sup>45–47</sup> on the chemisorption of gallium (Ga, Ga<sup>+</sup>)<sup>45</sup> and group IIIA nitrides on Si(111),<sup>45,47</sup> the electronic and geometric structure and the bonding of chemisorbed M on Si(111) are investigated using density functional theory (DFT) calculations and a Si<sub>26</sub>H<sub>22</sub> model of the Si(111) surface. The diffusion of M in the Si(111) surface is studied and the energy barriers between different stable structures are reported. Analysis and explanation of the differences among the different metal adsorbates are given.

## II. Computational Procedure

Cluster calculations have been used to determine the interaction of a single group IIIA metal atom M, M = B, Al, Ga, and In with the Si(111) surface. A 5-layer one-rest one-adatom (1R-1A) cluster model of Si(111) was constructed as previously detailed<sup>45,47,48</sup> using the dimer-adatom-stacking fault (DAS) structure<sup>49</sup> and the LEED data of Tong et al.<sup>50</sup> for the Si(111)-7 × 7 reconstructed surface. Hydrogen atoms (white spheres) have been added to terminate the 26-Si atom cluster (gray spheres = Si) at the sides as well as below the lowest Si level, while the adatom and rest atom are left with one dangling bond (i.e., one unpaired electron) each. Pictorially, the model cluster (clean Si(111)) is:



The model cluster approach of the present work compared to band structure calculations, where a periodic approach is employed and is considered to be appropriate because Si has localized bonds and states and the group III metal atom is

connected locally to the Si surface. Moreover the present approach is more convenient for the elucidation of the details of the movements of the metal atoms on the Si surface, which is one of the objectives of the present work.

DFT calculations were carried out using the B3LYP functional<sup>51,52</sup> and the DGDZVP basis set (double- $\zeta$  valence plus polarization, i.e., [3s2p1d<sub>B</sub>, N/4s3p1d<sub>Al, Si</sub>/5s4p2d<sub>Ga</sub>/6s5p3d<sub>In</sub>]).<sup>53</sup> This combination was considered to be the best choice for the present calculations, since the B3LYP/DGDZVP calculations on the diatomic molecules MN and MSi present satisfactory similarity with the best known ab initio calculations and experiments.<sup>47</sup> Moreover, the large size (49 atoms) of the systems calculated practically forbids the use of MRCI (multireference configuration interaction) or CC (coupled cluster) methods.

Additionally, calculations employing the Hay-Wadt LANL2DZ ECP<sup>54</sup> basis sets were performed in an effort to account for the relativistic effects, which might be of importance for Ga and In. These basis sets consist of a pseudopotential for the core electrons, up to 3d(4d) electrons of Ga(In), up to 2p electrons of Si and Al and a double- $\zeta$  quality basis set, for the three outer electrons of Al, Ga, and In, for the four outer electrons of Si, and the five electrons of B; i.e., (3s3p) → [2s2p]<sub>Al, Si, Ga, In</sub> and (10s5p) → [3s2p]<sub>B</sub>.

Eight chemisorbed structures for each of M-Si(111) were determined. Four of them (**a**, **b**, **c**, and **d**, see Figure 1) were found by energy optimization of the of M-Si(111) system with respect to the coordinates of the Si rest atom and Si adatom as well as those of the adsorbed species, in each case. The remaining cluster was kept fixed in order to retain the Si(111) surface structure. Structures **e–h** were determined as a result of the investigation of incorporation of the M in the Si cluster and the paths connecting the different extrema. In the process of these calculations it was found necessary to carry out more extensive optimizations than it was the case above for the **a–d** minima. Thus, the **a** and **e** structures were determined by energy optimization of the MSi<sub>2</sub>, MSi<sub>4</sub>, and MSi<sub>5</sub> subclusters in the M-Si<sub>26</sub>H<sub>22</sub> model of the metal chemisorbed Si(111) surface, involving the closest neighbors to M and Si adatom. Moreover, the replacement of the Si adatom by the metal (adsorption of the M atom at the T<sub>4</sub> and H<sub>3</sub> sites or **f** and **g** structures of Figure 1, respectively) and the substitution of the inner Si atom, directly below the Si adatom, with M (S<sub>5</sub> site, **h** structure) were investigated by energy optimization of the MSi<sub>3</sub>, MSi<sub>4</sub>, and MSi<sub>5</sub> subclusters in the model, while keeping the remaining cluster fixed in order to retain the Si(111) surface structure. Additionally, structure **b** was calculated by energy optimization of the MSi<sub>6</sub> subcluster in the model. Finally, the transition states between structures **a** and **e** (**i** transition state) and **f** and **g** (**j** transition state) were determined. More specifically, the path connecting the initial and the final structures was determined in each case by constrained optimizations of the coordinates of atoms 1, 2, 4, 5, 6, and 7 of Figure 1 (**a**, **e**, and **i**) for (**i**) and atoms 1, 3, 4, 5, 6, and 7 of Figure 1 (**f**, **g**, and **j**) for (**j**). For transition state **i**, the initial step at each point along the path involved determination of the vertical height for atoms 1 and 2 with respect to the surface by a series of single point calculations along that coordinate. In the next step, the coordinates of 4, 5, 6, and 7 atoms were optimized. Similarly for **j** at each point along the path, the vertical height of atom 1 with respect to the surface was energetically optimized and subsequently the coordinates of atoms 3, 4, 5, 6, and 7 were optimized.

All of the optimized minima (**a–h**) were verified that they are true minima: Given that it was not practical to calculate the

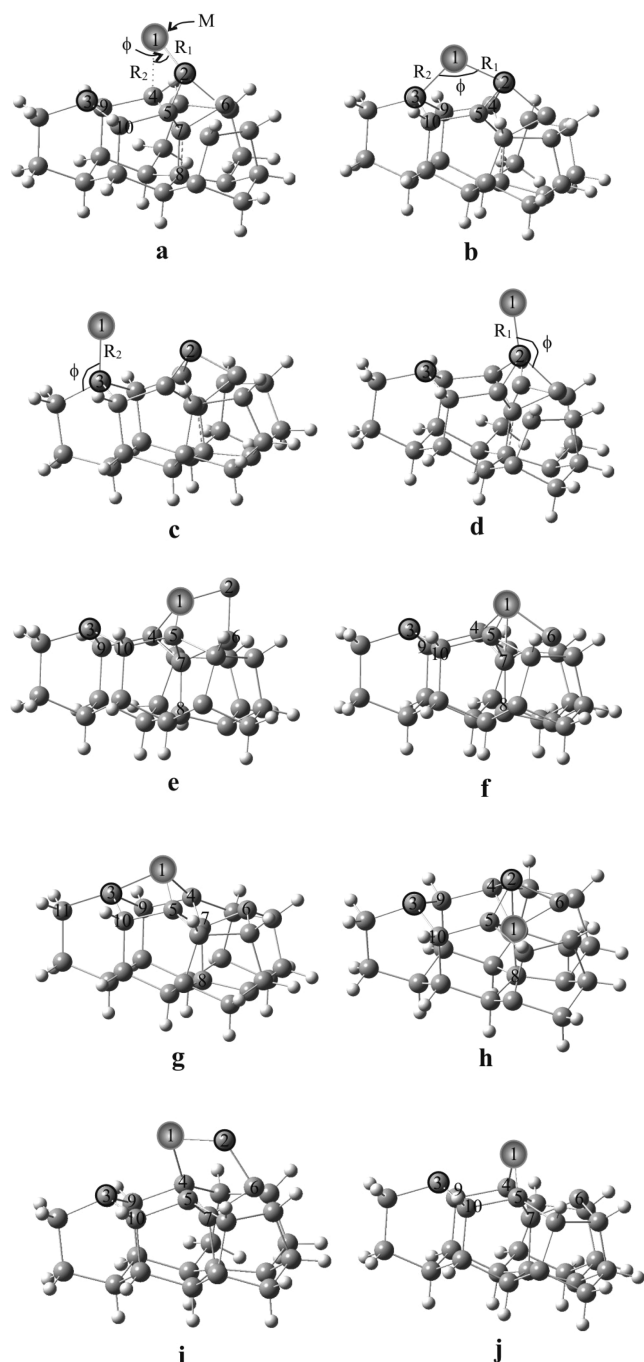


**Figure 1.** Eight stable structures (**a–h**) and two transition states structures (**i** and **j**) of  $M$ -Si(111),  $M = B, Al, Ga,$  and  $In$ . (Si = gray spheres,  $M$  = large gray spheres, and H = white spheres).

vibrational frequencies for a system of this size, we checked the potential energy surfaces around the minima. The metal atoms were shifted from the equilibrium position and geometry optimization was repeated. Similarly, additional points around the determined transition states (**i** and **j**) were calculated to check whether lower-energy transition structures could be determined. Thus there exists a good degree of confidence on the type of structures determined, minima and transition states.

Binding energy (BE) of each species to the surface was calculated for all stable geometries and the activation energy for the transition from **a** to **e** and from **f** to **g** were found. Moreover, for the sake of completeness, the basis set superposition error (BSSE) was estimated with respect to the

**TABLE 1: Geometry<sup>a</sup> ( $R$  (Å),  $\phi$  (degrees)), Net Charges  $q$ , and Binding Energies Corrected for BSSE  $BE_{BSSE}$  (eV) of the **a–d** Structures of  $M$ -Si(111),  $M = B, Al, Ga,$  and  $In$ , at the Early Stage of Adsorption, at B3LYP/DGDZVP Level of Theory**

structures	$R_1$	$R_2$	$\phi$	$q_1$	$q_2$	$q_3$	$BE_{BSSE}$	$BE_{BSSE}^b$
Si(111)					+0.22	+0.08		
<b>a-B</b>	1.97	2.07	80	-0.24	+0.27	+0.08	2.85	<sup>c</sup>
<b>a-Al</b>	2.52	2.84	58	+0.64	-0.25	+0.06	2.23	2.20
<b>a-Ga</b>	2.55	2.91	56	+0.59	-0.21	+0.06	2.13	2.14
<b>a-In</b>	2.75	3.24	50	+0.75	-0.32	+0.06	1.63	1.61
<b>b-B</b>	1.95	1.99	150	-0.20	+0.17	-0.02	2.80	3.04
<b>b-Al</b>	2.62	2.71	113	+0.84	-0.23	-0.41	2.21	2.13
<b>b-Ga<sup>d</sup></b>	2.93	2.77	102	+0.71	-0.09	-0.43	1.99 <sup>e</sup>	<sup>f</sup>
<b>b'-Ga<sup>d</sup></b>	3.07	2.67	102	+0.69	-0.02	-0.49	2.09 <sup>e</sup>	<sup>f</sup>
<b>b-In</b>	3.01	2.86	99	+0.79	-0.13	-0.49	2.06 <sup>e</sup>	<sup>f</sup>
<b>c-B</b>	2.10	111	+0.16	+0.22	-0.27	2.31	2.30	
<b>c-Al</b>	2.61	128	+0.68	+0.11	-0.62	2.20	2.26	
<b>c-Ga</b>	2.62	122	+0.63	+0.20	-0.57	2.10	2.09	
<b>c-In</b>	2.88	138	+0.72	-0.04	-0.57	1.91	1.93	
<b>d-B</b>	2.08	138	+0.16	-0.14	+0.08	2.18	<sup>c</sup>	
<b>d-Al</b>	2.57	141 <sup>g</sup>	+0.68	-0.49	+0.06	1.75	2.13	
<b>d-Ga</b>	2.58	141	+0.65	-0.42	+0.06	1.69	1.66	
<b>d-In</b>	2.77	133	+0.71	-0.50	+0.06	1.71	1.64	

<sup>a</sup> The energy optimization was done with respect to coordinates of  $M$ , Si-atom and Si-rest atom. <sup>b</sup> B3LYP/LANL2DZ. <sup>c</sup> The structure is not stable and it changes over to e-B-Si(111) cluster. <sup>d</sup> Equivalent, nearly identical structures. <sup>e</sup> The  $BE_{BSSE} = 2.08$  eV for **b-Ga**; 2.18 for **b'-Ga**; 2.15 for **b-In** when the energy optimization was done with respect to coordinates of seven atoms of the  $M$ -Si(111) structures; i.e., (1, 2, 3, 4, 5, 9, and 10), see Figure 1. <sup>f</sup> The structure is not stable and it changes over to c-M-Si(111) cluster. <sup>g</sup> The angle  $\phi$  can change from 128 to 141 degrees without significant change in energy.

relevant fragments by the counterpoise procedure.<sup>55,56</sup> All calculations were performed using the Gaussian 03 program package.<sup>57</sup>

### III. Results

Eight minima (**a–h**) and two transition-state structures (**i** and **j**) were determined for the  $M$ -Si(111) cluster,  $M = B, Al, Ga,$  and  $In$ , see Figure 1. They are labeled by the geometric structure, **a–j** followed by the name of the adsorbed species, for example, **a-B**, stands for the minimum corresponding to the **a** structure of Figure 1, for the B-Si(111) cluster. The  $M$ -Si(111) structures have been calculated for both doublet (one open shell electron) and quartet (three open-shell electrons) spin multiplicity. Given that the multiplicity has no meaning in a surface, we see that practically there is no difference in the geometry between the doublet and quartet  $M$ -Si(111) structures. However, there is generally only a slight difference in the total energy between the structures having doublet and quartet spin multiplicity. In this paper, only the lowest energy structures (geometry and multiplicity) are presented.

For  $M$ -Si(111), the geometries, binding energies corrected for BSSE, and natural population analysis (npa) of the structures determined are given in Tables 1 and 2, whereas the energy barriers for the transitions **a**  $\rightarrow$  **e** and **f**  $\rightarrow$  **g** are reported in Table 3. BSSE is small ranging between 0.01 and 0.1 eV, with the exception of the **h-Ga** and **h-In** structures where the BSSE is 0.2 and 0.3 eV, respectively. Generally, the B chemisorbed structures present the lowest BSSE, while the In chemisorbed structures the largest. The uncorrected for BSSE binding energies and energy barriers and more geometric data are given in the Supporting

**TABLE 2: Geometry<sup>a</sup> ( $R$  (Å),  $\phi$ (degrees)), Net Charges  $q$  of M or Si Atoms, and Binding Energies Corrected for BSSE  $BE_{BSSE}$ (eV) of the **a**, **e**, **f**(T<sub>4</sub>), **g**(H<sub>3</sub>), and **h**(S<sub>5</sub>) Structures of M–Si(111), M = B, Al, Ga, and In at B3LYP/DGDZVP Level of Theory**

	Si(111)	<b>a-B</b>	<b>a-Al</b>	<b>a-Ga</b>	<b>a-In</b>		Si(111)	<b>f-B</b>	<b>f-Al</b>	<b>f-Ga</b>	<b>f-In</b>
$R(1-2)$		1.95	2.54	2.57	2.76	$q_1$	+0.22	-0.76	+0.78	+0.55	+0.83
$R(1-4)$		2.02	2.79	2.85	3.05	$q_{4,5}$	-0.09	+0.18	-0.26	-0.18	-0.27
$R(2-4)$	2.44	2.87	2.67	2.68	2.70	$q_6$	-0.09	+0.21	-0.28	-0.20	-0.29
$R(7-8)$	2.18	2.36	2.32	2.33	2.33	$q_7$	-0.17	-0.06	-0.27	-0.26	-0.29
$\phi(4-1-2)$		93	60	59	55	$BE_{BSSE}^e$		4.83	3.04	2.53	2.00
$\phi(4-2-5)$	90	91	90	90	89	$BE_{BSSE}^f$		5.12	3.43	2.90	2.51
$\phi(4-7-5)$	93	104	101	101	101	$BE_{BSSE}^g$		5.12	3.43	2.90	2.54
$q_1$		-0.24	+0.62	+0.57	+0.69			<b>g-B<sup>g</sup></b>	<b>g-Al</b>	<b>g-Ga</b>	<b>g-In</b>
$q_2$	+0.22	+0.27	-0.19	-0.16	-0.23	$R(1-3)$			2.70	2.80	2.91
$q_4$	-0.09	+0.03	-0.35	-0.33	-0.37	$R(1-4)$			2.53	2.58	2.75
$BE_{BSSE}^b$		2.85	2.23	2.13	1.63	$R(3-11)$	2.37		2.51	2.50	2.47
$BE_{BSSE}^c$		2.92	2.28	2.17	1.96	$R(7-8)$	2.18		2.47	2.47	2.49
$BE_{BSSE}^d$		3.01	2.31	2.24	2.02	$\phi(3-1-5)$			94	91	87
$BE_{BSSE}^e$		3.21	2.51	2.36	2.19	$\phi(4-1-5)$			97	94	88
		<b>e-B</b>	<b>e-Al</b>	<b>e-Ga</b>	<b>e-In</b>	$\phi(4-7-5)$	93		106	107	108
$R(1-4)$	2.44	2.16	2.53	2.55	2.74	$q_1$		+0.88	+0.69	+0.91	
$R(1-2)$		1.94	2.44	2.41	2.63	$q_3$	+0.08		-0.33	-0.25	-0.31
$R(2-6)$		2.44	2.41	2.41	2.40	$q_{4,5}$	-0.09		-0.35	-0.27	-0.33
$R(7-8)$	2.18	2.28	2.38	2.38	2.41	$BE_{BSSE}^h$			2.09	1.70	1.51
$R(1-7)$	2.70	2.29	2.73	2.78	3.00	$BE_{BSSE}^i$			2.61	2.21	2.05
$\phi(4-1-5)$	90	109	94	92	86			<b>h-B</b>	<b>h-Al</b>	<b>h-Ga</b>	<b>h-In</b>
$\phi(4-7-5)$	93	98	104	103	105	$R(2-4)$	2.44	2.37	2.43	2.44	2.44
$\phi(1-2-6)$		70	72	74	75	$R(1-2)$	2.70	2.22	2.41	2.41	2.57
$q_1$		-0.96	+0.62	+0.37	+0.67	$R(1-4)$	2.39	2.09	2.44	2.42	2.62
$q_2$	+0.22	+0.58	+0.15	+0.21	+0.12	$R(1-8)$	2.18	2.04	2.32	2.28	2.46
$q_{4,5}$	-0.09	+0.16	-0.26	-0.19	-0.28	$R(1-6)$	2.38	2.13	2.51	2.52	2.68
$q_6$	-0.09	-0.08	-0.29	-0.24	-0.29	$\phi(4-2-5)$	90	93	102	101	104
$BE_{BSSE}^b$		4.27	2.01	1.51	1.06	$\phi(4-1-5)$	93	110	101	103	94
$BE_{BSSE}^c$		4.30	2.15	1.65	1.24	$\phi(8-1-6)$	122	110	119	115	127
$BE_{BSSE}^d$		4.40	2.40	1.91	1.62	$\phi(1-2-6)$	55	56	63	63	65
		<b>f-B</b>	<b>f-Al</b>	<b>f-Ga</b>	<b>f-In</b>	$q_1$	-0.17	-1.46	+0.84	+0.44	+0.94
$R(1-4)$	2.44	2.10	2.50	2.52	2.71	$q_2$	+0.22	+0.30	+0.09	+0.11	+0.04
$R(1-7)$	2.70	2.05	2.54	2.57	2.81	$q_{4,5}$	-0.09	+0.21	-0.32	-0.24	-0.32
$R(1-6)$	2.47	2.05	2.47	2.48	2.69	$q_6$	-0.09	+0.18	-0.25	-0.21	-0.31
$R(7-8)$	2.18	2.23	2.35	2.35	2.40	$q_8$	-0.20	+0.18	-0.49	-0.35	-0.36
$\phi(4-1-5)$	90	113	96	95	88	$BE_{BSSE}^d$		5.64	2.29	1.83	0.03
$\phi(7-1-6)$	55	72	57	57	52	$BE_{BSSE}^e$		6.26	2.30	1.83	0.19

<sup>a</sup> The energy optimization (EO) was done with respect to coordinates of six atoms of the M-Si(111) structures; i.e., **a** and **e** (1, 2, 4, 5, 6, 7); **f** and **g** (1, 3, 4, 5, 6, 7); **h** (1, 2, 4, 5, 6, 8). <sup>b</sup> EO with respect to coordinates of the (1, 2, 3) atoms. <sup>c</sup> EO with respect to coordinates of the (1, 2, 4) atoms. <sup>d</sup> EO with respect to coordinates of the (1, 2, 4, 5, 6) atoms. <sup>e</sup> EO with respect to coordinates of the (1, 3) atoms. <sup>f</sup> EO with respect to coordinates of the (1, 4, 5, 6, 7) atoms. <sup>g</sup> The g-B(H<sub>3</sub>) is not stable and its optimization leads to f-B(T<sub>4</sub>). <sup>h</sup> EO with respect to coordinates of the (1, 3, 4, 5) atoms.

**TABLE 3: Energy Barriers Corrected for BSSE  $EB_{BSSE}$ (eV) for the Transitions **a**  $\rightarrow$  **e** and **f**(T<sub>4</sub>)  $\rightarrow$  **g**(H<sub>3</sub>) of M–Si(111), M = B, Al, Ga, and In at B3LYP/DGDZVP Level of Theory**

structure	$EB_{BSSE}^a$	$EB_{BSSE}^a$
	<b>a <math>\rightarrow</math> i</b>	<b>i <math>\leftarrow</math> e</b>
<b>B–Si(111)</b>	0.49	1.67
<b>Al–Si(111)</b>	1.63	1.53
<b>Ga–Si(111)</b>	1.75	1.30
<b>In–Si(111)</b>	1.87	1.30
	<b>f(T<sub>4</sub>) <math>\rightarrow</math> j</b>	<b>j <math>\leftarrow</math> g(H<sub>3</sub>)</b>
<b>B–Si(111)<sup>b</sup></b>		
<b>Al–Si(111)</b>	1.25	0.44
<b>Ga–Si(111)</b>	1.10	0.40
<b>In–Si(111)</b>	0.67	0.20

<sup>a</sup> The energy optimization was done with respect to the coordinates of six atoms of the M-Si(111) structures; i.e., **a** and **e** (1, 2, 4, 5, 6, 7); **f** and **g** (1, 3, 4, 5, 6, 7). <sup>b</sup> Optimization of the g-B(H<sub>3</sub>) leads to f-B(T<sub>4</sub>).

Information. Moreover, it should be noted that there are no significant differences in geometry ( $R$ ,  $\phi$  of Figure 1), npa and BE between the results of B3LYP/DGDZVP and B3LYP/LANL2DZ calculations. Thus, only the B3LYP/DGDZVP

geometry and npa are given which we consider as our best results. In addition, for the BE, the B3LYP/LANL2DZ values are given, for comparison, for structures **a–d** in Table 1.

**A. a-M, b-M, c-M, and d-M Structures.** The **a–d** local minima (Figure 1) of the potential energy surface of chemisorbed M on Si(111) surface have the M atom residing atop the Si adatom, rest atom and in bridge position. At the minimum **a** the M atom is connected to the Si adatom at an angle so that it is directly above a second layer Si atom, adjacent to the adatom. In **b** M occupies a bridge position interacting with both the Si rest and Si adatom. In the next two stable structures (**c**, **d**), M is directly above the Si rest atom in the **c** and above the adatom in the **d** structure.

The geometry, the npa of the adsorbed M atoms and of the Si rest and Si adatom, and the BSSE corrected BE ( $BE_{BSSE}$ ) of structures **a–d** of M-Si(111) are given in Table 1. Graphically, the  $BE_{BSSE}$  values of the four minima (**a–d**) with respect to the M adsorbates are given in Figure 2. The results presented in Table 1 and Figure 2 have been obtained by energy optimization with respect to the coordinates of the Si rest atom and Si adatom as well as those of the adsorbed species; i.e., 1, 2, and 3 atoms

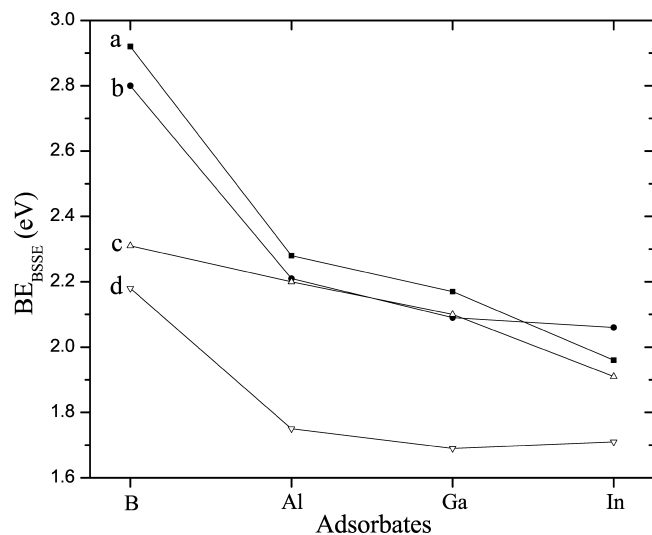


**Figure 2.** BSSE corrected binding energies  $BE_{BSSE}$  of the structures (a–d) with respect to the M adsorbates at B3LYP/DGDZVP level of theory. Geometry optimization of  $MSi_2$  within the  $Si_{26}H_{22}M$  cluster.

of Figure 1(a–d) while the remaining cluster was kept fixed in order to retain the Si(111) surface structure. The results of the additional optimization calculations (see above in the computational procedure section) on structures **a** for all M and **b** for Ga and In, are presented in Tables 1 and 2. As can be seen in Table 1 and Figure 2, as the atomic number increases the  $BE_{BSSE}$  of each structure decreases, with the exception of the **b** and **d** minima of adsorbed Ga and In which are practically the same. Moreover, it might be noted that the Al– and Ga–Si(111) structures have similarities in their geometry and the  $BE_{BSSE}$  values.

We observe that adsorbed B structures present the largest  $BE_{BSSE}$  (see Tables 1 and 2) and the shortest  $R_{M-Si}$  distances of the other adsorbates, for all four structures (a–d). The **a** minimum is the lowest of all adsorbed M among the a–d structures, where the metal is connected to the dangling bonds of the Si(111) surface. The  $BE_{BSSE}$  values are 3.21 (B), 2.51 (Al), 2.36 (Ga), and 2.19 (In) eV (see Table 2) when a subcluster  $MSi_5$  is relaxed, i.e., the energy optimization was done with respect to the coordinates of the  $MSi_5$ . For the In chemisorbed atom, the **a** structure is lower than **b** by 0.04 eV (2.19 (a) versus 2.15 (b) eV), when a subcluster  $MSi_5$  (a) and  $MSi_6$  (b) is relaxed while the ordering of **a** and **b** is reversed, when a smaller subcluster  $MSi_2$  is relaxed (see Tables 1 and 2). That shows that the energy optimization with respect to the coordinates of the largest subcluster is necessary.

As shown in Table 1, there is no significant difference in the  $BE_{BSSE}$  at B3LYP/DGDZVP and B3LYP/LANL2DZ level, for the Ga and In chemisorbed atom. The differences between the two levels of calculation are less than 0.07 eV.

Finally, in all the minimum energy structures of adsorbed Al, Ga, and In, according to the npa, the partial charges on M range from +0.59 to +0.84, with the Si surface withdrawing from M electron charge. For adsorbed B, in the **a** and **b** structures, B gains  $0.2 e^-$  while at the remaining **c** and **d** it loses  $0.2 e^-$ , cf. Table 1. The metal atom, for all M, in the **a**, **c**, and **d** structures is in its ground state  $^3P(s^2p)$ . The half-filled  $p_z$  orbital of M forms a bond with an  $sp^3$  orbital of the Si atom lying directly below. Charge, up to  $0.8 e^-$ , is transferred from M to Si, while there is a back-donation from the orbitals of the nearby Si atoms to the empty  $p_{x,y}$  orbitals of M ranging from 0.1 to  $0.7 e^-$ . In the **b** structure M seems to be a  $sp^2$  hybrid, in the  $^4P$  state.

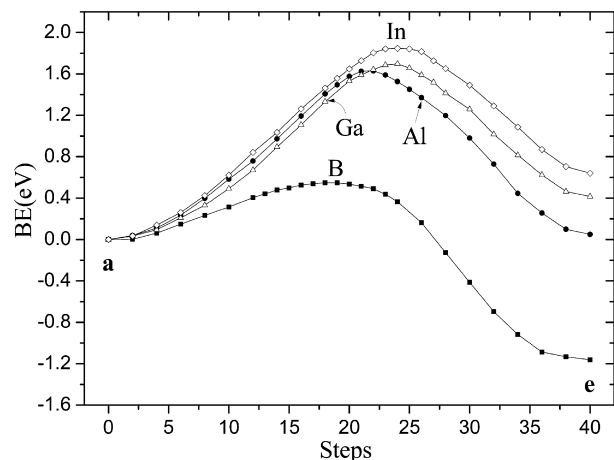


**Figure 3.** Potential energy curve during the movement of M from **a** to **e** structure at B3LYP/DGDZVP level of theory. The curves have been calculated with geometry optimization of  $Si_5M$  within the  $Si_{26}H_{22}M$  cluster and they have been shifted vertically so that the **a** structures are at 0. The steps are as discussed in the computational procedure.

**B. e-M, f-M, g-M, and h-M Structures.** At the e–h minima of the potential energy surface of chemisorbed M on Si(111) surface, the M atoms diffuse into the Si cluster and/or substitute Si atoms, see Figure 1.

At the **e-M** structure, the M atom substitutes the Si adatom of the Si cluster; the Si adatom is moved directly above a second layer Si atom, adjacent to the M atom. The  $BE_{BSSE}$  values are 4.40 (B), 2.40 (Al), 1.91 (Ga), and 1.62 (In) eV when a  $Si_5M$  subcluster is relaxed, see Table 2. The **e-B**–Si(111) cluster presents larger displacements than the other **e-M**–Si(111) with respect to the Si(111) surface because of the smaller distance of the B atom from the surface which results from the smaller size of the B atom, c.f. Table 2. The largest displacement,  $-0.4 \text{ \AA}$ , (with respect to the model Si(111) cluster) is found in the equilibrium distance between atoms 1 and 7 of Figure 1e, i.e., the distance between B and the Si atom lying directly below. For the case of In–Si(111), where In is the largest atom, the corresponding displacement is  $+0.3 \text{ \AA}$ , see Table 2.

The transition from structure **a** to structure **e** occurs through transition state structure **i**, see Figure 1. In all M–Si(111) with the exception of B–Si(111) the **a** structure is lower in energy than **e**. The calculated activation energy barriers from **a** to **e** are 0.5 (B), 1.6 (Al), 1.7 (Ga), and 1.9 eV (In) (see Table 3). The **a** → **e** barrier for B is significantly lower than the values of the other metals since **e** is the lowest energy structure along this path and the **e** → **a** barrier for B–Si(111) is 1.7 eV (see Table 3). Graphically, the potential energy curves for the M transfer from **a** to **e** structure at the B3LYP/DGDZVP level of theory are depicted for the different M in Figure 3.

A possible path from the **e** to the **f** structure would involve reconstruction of the surface/relocation of the Si atoms and it has not been possible to determine such a path in the present work. At the **f** structure the M atom takes the place of a Si adatom. It corresponds to the  $T_4$  adsorption site, while the **g** structure to the  $H_3$  site (see Figure 1). The BSSE corrected binding energies with respect to the clean Si(111) model cluster, for the **f** structure ( $T_4$ ) are  $BE_{BSSE} = 5.12$  (B), 3.43 (Al), 2.90 (Ga), and 2.54 eV (In), while for **g**( $H_3$ ) the  $BE_{BSSE}$  values are 2.61 (Al), 2.21 (Ga), and 2.05 eV (In), c.f. Table 2. Moreover, the desorption energy, the energy for the removal of the M chemisorbed from the **f** and **g** structures without reconstruction of the remaining Si cluster only with relaxation of the Si cluster are for the **f**( $T_4$ ) structure 5.86 (B), 4.17 (Al), 3.64 (Ga), and

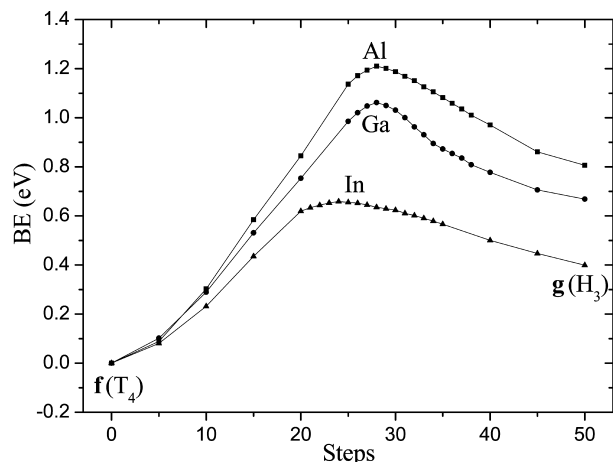


**Figure 4.** Potential energy curve during the movement of M from **f** to **g** structure at B3LYP/DGDZVP level of theory. The curves have been calculated with geometry optimization of  $\text{Si}_5\text{M}$  within the  $\text{Si}_{26}\text{H}_{22}\text{M}$  cluster and they have been shifted vertically so that the **f** structures are at 0. The steps are as discussed in the computational procedure.

3.27 eV (In), while for **g**( $\text{H}_3$ ) the corresponding values are 3.34 (Al), 2.94 (Ga), and 2.79 eV (In). It might be noted that for the case of boron, the **g**( $\text{H}_3$ ) structure is not stable and the optimization of **g**-**B** leads to **f**-**B**. Finally, the lowest energy structure is the **f** structure and the next higher structure is **g** for the Al, Ga and In chemisorbed atoms, while for boron the lowest energy structure is **h** (see below) and the next higher structure is **f**. The calculated activation energy barriers from **f** to **g** are 1.2 (Al), 1.1 (Ga), and 0.7 eV (In) (see Table 3). The transition state structure is the **j** structure, see Figure 1. Graphically, the potential energy curves during the M transfer from **f** to **g** structure at B3LYP/DGDZVP level of theory are depicted in Figure 4.

In Table 2 the geometries of the **f** and **g** structures are given and comparing the R distances between the metal chemisorbed structure and clean Si(111) it seems that the displacements are energetically favorable because they allow the Al and Ga adatom to move closer than the Si adatom to the Si surface, with the B adatom moving even closer because of its small size, while In is moving apart by 0.1 Å. Thus, the **f**-**B**-Si(111) is the most disturbed structure comparing to the other **f** structures. The largest displacement,  $-0.6$  Å, is the equilibrium distance between the B and the Si atom lying below, i.e., 1 and 7 atoms. More data concerning the geometry of the structures are given as Supporting Information.

In the **h** structure of Figure 1, the metal atom is found at a lower level of the surface, in the 5-fold coordinated substitutional site,  $\text{S}_5$ , directly below the Si adatom. The  $\text{BE}_{\text{BSSE}}$  of chemisorbed M at the **h** structure with respect to the Si(111) cluster are 6.26 (B), 2.30 (Al), 1.83 (Ga), and 0.19 (In) eV, see Table 2. Note that the uncorrected BE for BSSE for In is 0.52 eV, showing that more than half of its BE is BSSE. For the rest chemisorbed atom the BSSE is about 0.1 eV for B and Al and 0.2 eV for Ga. However, for the other structures of In the BSSE values range from 0.01 to 0.15 eV (see the Supporting Information for more details). For the In atom, the **h** structure is the highest energy of all other calculated structures. That fact shows that In does not prefer to diffuse inside to Si(111) but to be adsorbed in the top of the surface. On the other hand, the **h** structure is the lowest for the B chemisorbed atoms and B prefers to diffuse inside to Si(111). As also found for the other M-Si(111) structures, **h**-**B** presents the largest displacements among the different M. The largest displacement,  $-0.5$  Å, is

the equilibrium distance between the B and the Si adatom lying above, i.e., 1 and 2 atoms. For the remaining M atoms, the corresponding displacements range from  $-0.3$  to  $-0.1$  Å, see Table 2.

According to the npa analysis, the B atom in the **e**-**h** structures has a negative charge, it gains almost one electron from the Si surface, while the other three chemisorbed atoms (Al, Ga, and In) lose electronic charge and they have positive partial charges, see Table 2. However, all M seem to be  $\text{sp}^3$  hybridized. It might be noted that, in the **e** structure the 2-Si atom (see Figure 1e, originally the Si adatom) has an  $\text{s}^2\text{p}^2$  distribution.

Comparing our results on B-Si(111) with the previous studies, we found the **h** structure (substitutional  $\text{S}_5$ ) to be the lowest energy structure, as it has been reported in previous studies.<sup>2-7</sup> The bond distance B-Si adatom calculated at 2.22(2.30) Å by energy optimization of the coordinates of the 1, 2, 4, 5, 6, 8 (1, 2, 4, 5, 6) atoms, see Figure 1 and Table 2. The values are within the error bars of the experimental value of  $2.32 \pm 0.1$  Å.<sup>3</sup> The next lowest structure, **f** ( $\text{T}_4$  adsorption site), lies at 1.14 eV above **h**, c.f. Table 2, in agreement with the calculated corresponding value of 1 eV using local density functional slab calculations.<sup>4</sup> Wang et al.<sup>7</sup> using a small cluster  $\text{BSi}_5\text{H}_9$  found at B3LYP/6-31+G(3df,2p) level of theory BE of 7.49 eV for the **h** structure and 5.56 eV for **f** and their differences is 1.93 eV; while, using a  $\text{BSi}_{14}\text{H}_{21}$  cluster found at B3LYP/6-31G\* level of theory BE of 7.21 eV for the **h** structure. Our corresponding values are smaller and mainly for the **h** structure, 6.26 (**h**) and 5.12 (**f**) eV because our cluster ( $\text{BSi}_{26}\text{H}_{22}$ ) is larger than theirs and for the  $\text{S}_5$  substitutional site a larger cluster of 5 layers seems to be needed.

In the case of Al chemisorbed atom, the  $\text{T}_4$  adsorbed site (cf. our structure **f**) is our lowest energy structure followed by the  $\text{H}_3$  adsorbed site (cf. structure **g**) as also found previously in the literature.<sup>8-10,12,15,18</sup> The difference between the two structures is found to be 0.82 eV, in agreement with the value of Illas et al.<sup>9</sup> of 0.81 eV at CI/DZP level of theory. Other theoretical studies applying band structure calculations,<sup>8</sup> DFT cluster calculations,<sup>12a</sup> and MP2<sup>10</sup> found the difference to be around 0.2–0.3 eV, while, band structure calculations with the Car-Parrinello method calculated the difference at 0.56 eV.<sup>20</sup> The calculated binding energy of Al at the  $\text{T}_4$  site is reported in the literature to range from 0.7 (HF) to 5.6 eV (band structure calculation) with the best given values or estimated values at 2.08 (CI/DZP),<sup>9</sup> 4.4 (estimated MP2 value),<sup>10</sup> 5.4 (band structure calculation),<sup>22</sup> and 5.6 eV (band structure calculation).<sup>8</sup> Our best value for the binding energy of Al at the  $\text{T}_4$  site is 3.43 eV. We found for the migration process of an Al adatom from  $\text{T}_4$  to  $\text{H}_3$ , activation energy of 1.2 eV which is comparable to the value of 0.9 eV of Hoshino et al.<sup>12a</sup> who performed DFT cluster calculations using the  $1 \times 1$  unreconstructed surface. For the  $\text{T}_4$  site, our calculated bond length between the Al and the second layer Si atom,  $R(1-7)$  is 2.54 Å, the CI/DZP gives 2.535 Å,<sup>9</sup> the MP2/ECP-DZ 2.398,<sup>10</sup> and the band structure calculations give 2.63 Å.<sup>8</sup> For the  $\text{H}_3$  site, the calculated bond length between the Al and the three surface Si atoms,  $R(1-4) = R(1-5) = 2.53$  and  $R(1-3) = 2.70$  Å, while the band structure calculations give 2.53 Å for all three bond distances. Comparing our calculated geometry with a LEED analysis of the Si(111)- $(\sqrt{3} \times \sqrt{3})\text{R}30^\circ$ -Al structure<sup>18</sup> we found small differences 0–0.1 Å; i.e., theory (expt<sup>18</sup>):  $R(1-7) = 2.54(2.49)$ ,  $R(7-6) = 2.41(2.41)$ ,  $\text{S}_5$ :  $R(1-8) = 2.32(2.23)$ ,  $R(1-6) = 2.51(2.41)$ , and  $R(2-6) = 2.39(2.49)$  Å.

Comparing our results on chemisorbed Ga and the data from the literature there is agreement on that the  $T_4$  adsorbed site is the lowest energy structure.<sup>15,24</sup> Our geometry for the **f** structure is in agreement with the results of the LEED analysis;<sup>28</sup> i.e.,  $R(1-6) = 2.48(2.50)$ <sup>28</sup>  $R(6-7) = 2.40(2.43)$ .<sup>28</sup> The energy difference between the  $T_4$  and  $H_3$  adsorption site is 0.69 while band structure calculations give 0.38 eV.<sup>15</sup> Experimentally, the  $(\sqrt{3} \times \sqrt{3})R30^\circ$  electron diffraction pattern observed with 1/3 monolayer coverage, is consistent with the Ga adatoms lying at a distance of  $1.49 \pm 0.03$  Å above the bulk extrapolated surface (111) plane.<sup>29</sup> Band structure calculations predict this distance at 1.33 Å,<sup>29</sup> while our study calculated the Ga 1.41 Å above the bulk (111) plane. Band structure calculations give BE of 4.2 eV<sup>22</sup> while our calculations give a smaller value of 2.90 Å for the **f** structure ( $T_4$  adsorption site). Thundat et al.<sup>30</sup> using small  $\text{GaSi}_m\text{H}_n$  clusters having 3 to 9 Si atoms found at HF/STO-3G level BE = 7.76 (**f**), 2.0 (**g**), 6.05 (**c**, **d**), and 4.0 eV (**h**). These values differ from ours of 2.90 (**f**), 2.21 (**g**), 2.09 (**c**), and 1.83 eV (**h**) because their clusters are smaller and not sufficient for the calculation of the BE values. However, their optimized Ga-Si bond distances are in relative agreement with ours, the differences between their Ga-Si bond distances and ours are up to 0.13 Å. Finally, Cho et al.<sup>31</sup> and Lee et al.<sup>14</sup> using band structure calculations give data in total for 6 and 7 adsorption sites, respectively, with the M atom located above the Si surface around the Si rest atom; these sites are different from the lowest  $T_4$  and  $H_3$  adsorption sites (**f** and **g** structures). They found binding energies ranging from 3.36 to 2.55 eV<sup>31</sup> and from 2.58 to 2.48 eV.<sup>14</sup> For the **b** and **c** structures, they found 3.09,<sup>31</sup> 2.48,<sup>14</sup>(**b**) and 2.55<sup>31</sup> eV (**c**). Our corresponding values are 2.18 (**b**) and 2.09 eV (**c**). It was not possible to reproduce their calculations on some adsorption sites due to convergence problems of the geometry optimization at the particular structures.

Finally, in the case of In, the energy difference between the  $T_4$  and  $H_3$  adsorption sites are calculated here at 0.49 while band structure calculations give 0.2 eV.<sup>15</sup> Lee et al.<sup>14</sup> calculated BE = 2.38 eV for the **b** structure in agreement with our calculated  $\text{BE}_{\text{BSSE}}$  of 2.15 eV. Some of their adsorption sites were not found to lead to stable geometrical structures in our calculations. Krausch et al.<sup>37</sup> using the PAC spectroscopy estimated the BE of In atom in the  $T_4$  structure to be 1.93(10) eV, whereas Baba et al.<sup>33</sup> found a larger BE by RHEED techniques: They studied isothermal In desorption from In superstructures formed on Si(111) at In coverages of 0.2–0.45 ML and found binding energy of 2.73(8) and at In coverages of 0.45–0.8 ML 2.86(8) eV.<sup>33</sup> Our corresponding calculated binding energy for the **f** structure is 2.54 eV between the experimental values of 1.93(10)<sup>37</sup> and 2.73(8) eV.<sup>33</sup> The ICISS technique<sup>36</sup> and the X-ray diffraction study<sup>38</sup> indicate the  $T_4$  adsorption site as the more appropriate and their best fit models indicate that the geometry is  $R(1-4) = 2.6 \pm 0.2$ <sup>36</sup> (2.58<sup>38</sup>) and  $R(1-7) = 2.68 \pm 0.15$ <sup>36</sup> (2.77<sup>38</sup>) Å. Our corresponding bond distances,  $R(1-4) = 2.71$  and  $R(1-7) = 2.81$  Å are within the error bars of these experimental values. Lin et al.<sup>41</sup> and Yoon et al.<sup>42</sup> used STM and STS techniques to study the initial stages of room-temperature deposition of In on Si(111)  $7 \times 7$  surface and observed individual In atoms residing atop the substrate Si adatoms (**d** structure)<sup>41,42</sup> and Si rest atoms (**c** structure),<sup>41,42</sup> and substitution of In for Si atoms in the  $7 \times 7$  adatoms position (**f** structure).<sup>42</sup>

To summarize, the present work is generally in good agreement with existing previous work. In particular, our results are in good agreement with experimental work, where available,

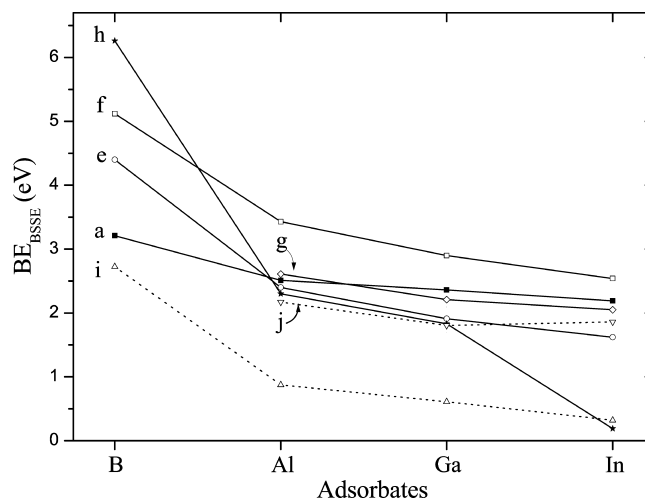


**Figure 5.** BSSE corrected binding energies  $\text{BE}_{\text{BSSE}}$  of the structures (**a**, **e**, **f**, **g**, **h**, **i**, and **j**) with respect to the M adsorbates at B3LYP/DGDZVP level of theory. Geometry optimization of  $\text{MSi}_5$  within the  $\text{Si}_{26}\text{H}_{22}\text{M}$  cluster.

concerning geometries and binding energies, showing that the model cluster approach of the present work is appropriate for the study of such systems. Moreover, our geometries are in good agreement with the geometries found with band structure calculations. Some band structure calculations calculate larger BE than our values for some structures. Additionally, comparing our results with previous studies, it seems that a 5-layer Si (or at least a 4-layer) cluster model of the Si(111) surface is necessary in order to retain the Si(111) surface structure. When smaller cluster were used and full optimization were applied the results in the BE values were not very good, while, the geometry seems to be effected less than the BE by the use of a small cluster.

Graphically, the BSSE corrected binding energies  $\text{BE}_{\text{BSSE}}$  of the stable structures (**a**, **e**, **f**, **g**, and **h**) and the transition state structures (**i** and **j**) with respect to the M adsorbates at B3LYP/DGDZVP level of theory are given in Figure 5. As shown the binding energy decreases with increasing size of the chemisorbed atom, with the  $\text{BE}_{\text{BSSE}}$  values of the B-Si(111) structures being significantly larger than the corresponding values of the other M structures. With the exception of the **h** structure which is only slightly bound for adsorbed In, the differences of  $\text{BE}_{\text{BSSE}}$  of the Al, Ga, and In chemisorbed metal at the different stable structures are small, ranging from 0.3 to 0.9 eV.

#### IV. Conclusions

The electronic and geometric structures of group IIIA elements (M) adsorbed on Si(111),  $M = \text{B}, \text{Al}, \text{Ga}$ , and In were studied by DFT calculations and a 5-layer, 1 rest atom and 1 adatom Si cluster model of the Si(111) surface, terminated with H atoms. Eight stable structures were determined for the M and two transition state structures. Moreover, the lowest energy paths connected stable structures are given for all M metals for the first time with the exception of the path connecting the **f**( $T_4$ ) and **g**( $H_3$ ) structures of Al chemisorbed atom. Our results are summarized as follows:

1. The adsorbed B structures have the largest  $\text{BE}_{\text{BSSE}}$  (binding energy corrected for the basis set superposition error) and the shortest  $R_{\text{M-Si}}$  distances among the M adsorbates. Moreover, B-Si(111) presents larger displacements than the remaining M-Si(111) compared to the clean Si(111).

2. The BE<sub>BSE</sub> of the lowest calculated M–Si(111) structures are: 6.26 (B, 5-fold coordinated substitutional site), 3.43 (Al, T<sub>4</sub> adsorption site), 2.90 (Ga, T<sub>4</sub>), 2.54 eV (In, T<sub>4</sub>) at the B3LYP/DGDZVP level of theory. The next lowest calculated M–Si(111) structures are a T<sub>4</sub> adsorption site for B and a H<sub>3</sub> adsorption site for the rest metals.

3. The B metal prefers to diffuse below the surface and obtain an S<sub>5</sub> substitutional site below the Si T<sub>4</sub> adatom because it has the smaller size than the other group IIIA metal. On the other hand the other three metals prefer to be chemisorbed at a T<sub>4</sub> adsorption sites and for the In atom which has the largest size, the substitutional S<sub>5</sub> adsorption site is only a slightly bound structure.

4. The H<sub>3</sub> adsorption site for the B atom is not stable.

5. The activation energy barriers from **a** (the M atom is connected to Si adatom at an angle so that it is directly above a second layer Si atom, adjacent to the adatom) to **e** (precursor of the T<sub>4</sub> adsorption site, the M atom substitutes the Si adatom of the Si cluster; the Si adatom is moving directly above a second layer Si atom, adjacent to the M atom) are estimated to be 0.5 (B), 1.6 (Al), 1.7 (Ga), and 1.9 eV (In).

6. The calculated activation energy barriers from **f**(T<sub>4</sub> adsorption site) to **g**(H<sub>3</sub> adsorption site) are estimated to be 1.2 (Al), 1.1 (Ga), and 0.7 eV (In).

7. According to the natural population analysis almost in all calculated structures, the B atom pulls electron charges from the surface, while the remaining metals donate electron charges to the surface. This is in agreement with the fact that B has larger electronegativity than the Si atoms and the remaining metals have smaller.

The present work is generally in good agreement with previous work where available. Moreover, it completes the studies which already exist on the chemisorption of group IIIA metal on Si(111). It reports data for all B, Al, Ga, and In chemisorbed metal with the same methodology, concerning not only the lowest energy structures but also some other structures. Comparisons are reported and explanations for the differences are given.

**Acknowledgment.** Financial support from the EU FP7, Capacities Program, NANOHOST project (GA 201729) is acknowledged.

**Supporting Information Available:** Additional tables of calculated data. This material is available free of charge via the Internet at <http://pubs.acs.org>.

## References and Notes

- (1) See for instance Wang, Y.; Schmidt, V.; Senz, S.; Gösele, U. *Nat. Nanotechnol.* **2006**, *1*, 186.
- (2) Headrick, R. L.; Robinson, I. K.; Vlieg, E.; Feldman, L. C. *Phys. Rev. Lett.* **1989**, *63*, 1253.
- (3) Huang, H.; Tong, S. Y.; Quinn, J.; Jona, F. *Phys. Rev. B* **1990**, *41*, 3276.
- (4) Avouris, P.; Lyo, I.-W.; Bozco, F.; Kaxiras, E. *J. Vac. Sci. Technol. A* **1990**, *8*, 3405.
- (5) Kumagai, Y.; Mori, R.; Ishimoto, K.; Hasegawa, F. *Jpn. J. Appl. Phys.* **1994**, *33*, L817.
- (6) Lyo, I.-W.; Kaxiras, E.; Avouris, P. *Phys. Rev. Lett.* **1989**, *63*, 1261.
- (7) Wang, S.; Radny, M. W.; Smith, P. V. *J. Phys.: Condens. Matter* **1997**, *9*, 4535.
- (8) Northrup, J. E. *Phys. Rev. Lett.* **1984**, *53*, 683.
- (9) (a) Illas, F.; Ricart, J. M.; Casanovas, J.; Rubio, J. *Surf. Sci.* **1992**, *275*, 459. (b) Rubio, J.; Illas, F.; Ricart, J. M. *Phys. Rev. B* **1988**, *38*, 10700. (c) Illas, F.; Ricart, J. M.; Rubio, J.; Casanovas, J. *Phys. Rev. B* **1993**, *47*, 2417.
- (10) Kairys, V.; Head, J. D. *Surf. Sci.* **1997**, *380*, 283.
- (11) Akpati, H. C.; Nordlander, P.; Lou, L.; Avouris, P. *Surf. Sci.* **1997**, *372*, 9.
- (12) (a) Hoshino, T.; Okano, K.; Enomoto, N.; Hata, M.; Tsuda, M. *Surf. Sci.* **1999**, *423*, 117. (b) Enomoto, N.; Hoshino, T.; Hata, M.; Tsuda, M. *Appl. Surf. Sci.* **1998**, *130*, 237.
- (13) Zhang, L.; Zhang, S. B.; Xue, Q.-K.; Jia, J.-F.; Wang, E. G. *Phys. Rev. B* **2005**, *72*, 033315.
- (14) Lee, G.; Kim, J. S. *Comput. Phys. Commun.* **2007**, *177*, 44.
- (15) Nicholls, J. M.; Reihl, B.; Northrup, J. E. *Phys. Rev. B* **1987**, *35*, 4137.
- (16) Uchida, H.; Kuroda, T.; Mohamad, F.; Kim, J.; Nishimura, K.; Inoue, M. *Surf. Sci.* **2004**, *566*, 197.
- (17) Hamers, R. J.; Demuth, J. E. *Phys. Rev. Lett.* **1988**, *60*, 2527.
- (18) Huang, H.; Tong, S. Y.; Yang, W. S.; Shih, H. D.; Jona, F. *Phys. Rev. B* **1990**, *42*, 7483.
- (19) Schwennicke, C.; Wang, X.-S.; Einstein, T. L.; Williams, E. D. *Surf. Sci.* **1998**, *418*, 22.
- (20) Tsuge, H.; Arai, M.; Fujiwara, T. *Jpn. J. Appl. Phys.* **1991**, *30*, L1583.
- (21) Lander, J.; Morrison, J. *Surf. Sci.* **1964**, *2*, 553. *Appl. Phys.* **1965**, *36*, 1706.
- (22) Matsuo, Y.; Kangawa, Y.; Togashi, R.; Kakimoto, K.; Koukitu, A. *J. Cryst. Growth* **2007**, *300*, 66.
- (23) Bolmont, D.; Chen, P.; Sébenne, C. A.; Proix, F. *Surf. Sci.* **1984**, *137*, 280.
- (24) Nogami, J.; Park, S.; Quate, C. F. *Surf. Sci.* **1988**, *203*, L631.
- (25) Gallas, B.; Berbezier, I.; Chevrier, J.; Derrien, J. *Phys. Rev. B* **1996**, *54*, 4919.
- (26) Čechal, J.; Kolíbal, M.; Kostelník, P.; Šikola, T. *J. Phys.: Condens. Matter* **2007**, *19*, 016011.
- (27) Morita, M.; Takeda, S. N.; Yoshikawa, M.; Kuwako, A.; Kato, Y.; Daimon, H. *Appl. Surf. Sci.* **2008**, *254*, 7872.
- (28) Kawazu, A.; Sakama, H. *Phys. Rev. B* **1988**, *37*, 2704.
- (29) Zegenhagen, J.; Patel, J. R.; Freeland, P.; Chen, D. M.; Golovchenko, J. A.; Bedrossian, P.; Northrup, J. E. *Phys. Rev. B* **1989**, *39*, 1298.
- (30) Thundat, T.; Mohapatra, S. M.; Dev, B. N.; Gibson, W. M.; Das, T. P. *J. Vac. Sci. Technol.* **1998**, *6*, 681.
- (31) Cho, K. N.; Kaxiras, E. *Surf. Sci.* **1998**, *396*, L261.
- (32) Tsay, S.-F.; Tsai, M.-H.; Lai, M. Y.; Wang, Y. L. *Phys. Rev. B* **2000**, *61*, 2699.
- (33) Baba, S.; Kawaji, M.; Kinbara, A. *Surf. Sci.* **1979**, *85*, 29.
- (34) Kawaji, M.; Baba, S.; Kinbara, A. *Appl. Phys. Lett.* **1979**, *34*, 748.
- (35) Nogami, J.; Park, S.; Quate, C. F. *Phys. Rev. B* **1987**, *36*, 6221.
- (36) Cornelison, D. M.; Chang, C. S.; Tsong, I. S. T. *J. Vac. Sci. Technol. B* **1990**, *8*, 3443.
- (37) Krausch, G.; Detzel, T.; Fink, R.; Luckscheiter, B.; Platzter, R.; Wöhrmann, U.; Schatz, G. *Phys. Rev. Lett.* **1992**, *68*, 377.
- (38) Finney, M. S.; Norris, C.; Howes, P. B.; van Silfhout, R. G.; Clark, G. F.; Thornton, J. M. C. *Surf. Sci.* **1993**, *291*, 99.
- (39) Krausch, G.; Fink, R.; Jacobs, K.; Luckscheiter, B.; Lohmüller, J.; Runge, B.-U.; Wöhrmann, U.; Schatz, G. *Surf. Sci.* **1993**, *285*, 81.
- (40) Öfner, H.; Surnev, S. L.; Shapira, Y.; Netzer, F. P. *Phys. Rev. B* **1993**, *48*, 10940.
- (41) Lin, X. F.; Mai, H. A.; Chizhov, I.; Willis, R. F. *J. Vac. Sci. Technol. B* **1996**, *14*, 995.
- (42) Yoon, M.; Willis, R. F. *Surf. Sci.* **2002**, *512*, 255.
- (43) Sun, M.; Hu, C.; Zhao, R. G.; Ji, H. *Thin Solid Films* **2005**, *489*, 111.
- (44) Byun, J. H.; Ahn, J. R.; Choi, W. H.; Kang, P. G.; Yeom, H. W. *Phys. Rev. B* **2008**, *78*, 205314.
- (45) Tzeli, D.; Petsalakis, I. D.; Theodorakopoulos, G. *Chem. Phys. Lett.* **2007**, *448*, 88.
- (46) Tzeli, D.; Theodorakopoulos, G.; Petsalakis, I. D. *Frontiers in Quantum Systems in Chemistry and Physics - PTCP*, **2008**, *18*, 341. *Proceedings of the QCSP-XII, London 2007*; Wilson, S.; Grout, P. J.; Maruani, J.; Delgado-Barrio, G.; Piecuch, P., Eds.; Springer Science: New York, 2008; Vol. 18, p 341.
- (47) Tzeli, D.; Petsalakis, I. D.; Theodorakopoulos, G. *J. Phys. Chem. C* **2009**, *113*, 5563.
- (48) Hari Kumar, K. R.; Petsalakis, I. D.; Polanyi, J. C.; Theodorakopoulos, G. *Surf. Sci.* **2004**, *572*, 162.
- (49) Takayanagi, K.; Tanishiro, Y.; Takahashi, M.; Takahashi, S. *J. Vac. Sci. Technol. A* **1985**, *3*, 1502.
- (50) Tong, S. Y.; Huang, H.; Wei, C. M. *J. Vac. Sci. Technol. A* **1988**, *6*, 615.
- (51) Becke, A. D. *J. Chem. Phys.* **1993**, *98*, 1372.
- (52) Lee, C.; Yang, W.; Parr, R. G. *Phys. Rev. B* **1988**, *37*, 785.
- (53) Godbout, N.; Salahub, D. R.; Andzelm, J.; Wimmer, E. *Can. J. Chem.* **1992**, *70*, 560.
- (54) Hay, P. J.; Wadt, W. R. *J. Chem. Phys.* **1985**, *82*, 299.
- (55) Boys, S. F.; Bernardi, F. *Mol. Phys.* **1970**, *19*, 553.
- (56) Tzeli, D.; Mavridis, A.; Xantheas, S. *J. Phys. Chem. A* **2002**, *106*, 11327.
- (57) Frisch, M. J.; Trucks, G. W.; Schlegel, H. B.; Scuseria, G. E.; Robb, M. A.; Cheeseman, J. R.; Montgomery, J. A., Jr.; Vreven, T.; Kudin, K. N.;

Burant, J. C.; Millam, J. M.; Iyengar, S. S.; Tomasi, J.; Barone, V.; Mennucci, B.; Cossi, M.; Scalmani, G.; Rega, N.; Petersson, G. A.; Nakatsuji, H.; Hada, M.; Ehara, M.; Toyota, K.; Fukuda, R.; Hasegawa, J.; Ishida, M.; Nakajima, T.; Honda, Y.; Kitao, O.; Nakai, H.; Klene, M.; Li, X.; Knox, J. E.; Hratchian, H. P.; Cross, J. B.; Adamo, C.; Jaramillo, J.; Gomperts, R.; Stratmann, R. E.; Yazyev, O.; Austin, A. J.; Cammi, R.; Pomelli, C.; Ochterski, J. W.; Ayala, P. Y.; Morokuma, K.; Voth, G. A.; Salvador, P.; Dannenberg, J. J.; Zakrzewski, V. G.; Dapprich, S.; Daniels, A. D.; Strain, M. C.; Farkas, O.; Malick, D. K.; Rabuck, A. D.;

Raghavachari, K.; Foresman, J. B.; Ortiz, J. V.; Cui, Q.; Baboul, A. G.; Clifford, S.; Cioslowski, J.; Stefanov, B. B.; Liu, G.; Liashenko, A.; Piskorz, P.; Komaromi, I.; Martin, R. L.; Fox, D. J.; Keith, T.; Al-Laham, M. A.; Peng, C. Y.; Nanayakkara, A.; Challacombe, M.; Gill, P. M. W.; Johnson, B.; Chen, W.; Wong, M. W.; Gonzalez, C.; Pople, J. A. *Gaussian 03*, revision C.02; Gaussian, Inc.: Wallingford CT, 2004.

JP903389R